Liquid phase hydrogenation of crotonaldehyde over copper incorporated in MCM-48

Victoria Gutierrez [a], Mariana Dennehy [b], Alejandra Diez [b], María A. Volpe [a,*]

[a] *Planta Piloto de Ingeniería Química, Camino Carrindanga Km7, CP 8000 Bahía Blanca, Argentina*
[b] *INQUISUR, Departamento de Química, Universidad Nacional del Sur, Avenida Alem 1253, CP 8000 Bahía Blanca, Argentina*

ARTICLE INFO

ABSTRACT

A series of Cu/MCM-48 catalysts is studied for the liquid phase hydrogenation of crotonaldehyde. Copper is incorporated in MCM-48 following a classical hydrothermal synthesis or by wet impregnation of the MCM-48 precursor (before eliminating the directing agent) with $Cu(AcAc)_2$. The copper loading is in the 2–20 wt% range. Characterization results from TPR and XRD indicate that copper crystals supported on MCM-48 surface coexist with copper incorporated in the MCM-48 walls. The presence of Cu^+ in MCM-48 is concluded from characterization with FTIR of adsorbed CO. This species would be the responsible for the relatively high selectivity of Cu/MCM-48. These catalysts show approximately 50% of selectivity against 7% of Cu/SiO_2 (both values measured at 10% of conversion).

© 2012 Elsevier B.V. All rights reserved.

1. Introduction

Copper on MCM-41 has been widely employed as catalysts for different reactions [1–11]. On the contrary copper supported on MCM-48 has been much less studied, though this system should be preferred to the one supported on MCM-41 in the basis of the three dimensional structure of MCM-48. Probably this is due the fact that it is rather difficult to incorporate a high copper loading to the mesoporous structure of MCM-48 [12].

In a previous work [13] we have studied a series of copper catalysts employing MCM-48 as the support for the selective hydrogenation of cinnamaldehyde in liquid phase. Some of these samples were found to be more selective than copper supported on silica or alumina. It is well known that is very difficult to hydrogenate carbonyl bond in α, β-unsaturated compounds, due to kinetic and thermodynamic difficulties. In this context, our previous results encouraged us to further investigate on the catalytic properties of Cu/MCM-48 for selective hydrogenation reactions.

In the present work we study a series of Cu/MCM-48, for the liquid phase hydrogenation of crotonaldehyde. This α,β-unsaturated compound has been selected since it presents a low steric protection of the olefinic bond, then, hydrogenation of crotonaldehyde is still a big challenge for researchers.

The samples are studied by FTIR of adsorbed CO, XRD, TPR and BET. Finally, the samples are tested in the liquid phase hydrogenation of crotonaldehyde, in a Batch reactor. The catalytic patterns are discussed in the light of the characterization results.

2. Experimental

2.1. Catalyst preparation

2.1.1. Synthesis of MCM-48

The silicon source was tetraethyl ortho-silicate (TEOS, Aldrich). The structure-directing agent was cetyltrimethylammoniun bromide (CTAB, Aldrich). MCM-48 was prepared by hydrothermal synthesis, following the technique reported by Xu et al. [14]. 10 mL of TEOS were added to a solution of CTAB in water (8.8 g/79.2 mL). 10 mL of NaOH 2 M were added at 308 K. The mixture was stirred for half an hour. The gel was heated to 373 K for 72 h under static hydrothermal conditions in a steel/Teflon autoclave. The product was filtered, washed with water, and dried at room temperature. Finally the solid was heated up 673 K at 0.5 K min^{-1} under N_2 flow, afterwards the flow was switched to chromatographic air, and the temperature was kept constant for 6 h.

2.1.2. Synthesis of Cu/MCM-48

Two series were prepared, one of them following a hydrothermal synthesis and another one by wet impregnation of MCM-48 with $Cu(AcAc)_2$.

The first series was prepared by following a classical hydrothermal method. The samples are named as CuH*x*, where *x* corresponds approximately to the copper wt%. A solution of $Cu(NO_3)_2$ (in 27% aqueous ammonia) was added to a solution of CTAB, NaOH and TEOS. Copper nitrate solutions with different concentration were employed in order to vary the metal content. The mixture was stirred for 4 h, before loading the sample into a Teflon-steel autoclave. The solution was heated for 3 days at 373 K. The product was then filtered and washed and finally treated for eliminating the structure directing agent, in the same way as in the preparation of pure MCM-48. The copper metal loading was measured by AAS. Three samples were obtained: CuH2, CuH3 and CuH5.

The other series, Cu*Ix* (where *x* corresponds approximately to the copper wt%) was prepared by wet impregnation of MCM-48, before performing the elimination of CTBA as it is conventionally carried out (with a calcination pre-treatment). This solid was put in contact with different solutions of $Cu(AcAc)_2$ in tetrahidrofuran for 24 h. The concentration of the solutions was varied in order to obtain a copper concentration of approximately 5, 10 and 20%. The solids were filtered, and dried at 343 K during 4 h. Afterwards the temperature was increased at 1°/min up to 673 K, under N_2 flow. At this temperature, the gas flow was switched to chromatographic air and the sample was calcined for 6 h. Three samples were obtained: CuI4, CuI9 and CuI20.

2.1.3. Synthesis of Cu/SiO₂

The support was SiO_2, from Rhône Poulenc (99.7%, Na: 0.1%, $SO4_2$: 0.1%, others: 0.1%), with a BET surface area of 210 m²/g. The silica was comprised of 3 mm diameter spheres. Copper was fixed to silica following a wet impregnation with solutions of $Cu(AcAc)_2$ (Aldrich, 99.99%) in THF. The support was calcined at 300 °C, and afterwards it was put in contact with a $Cu(AcAc)_2$ solution for 48 h, at 60 °C, under constant stirring. The solid was filtered and heated at 70 °C for 24 h. Finally the sample was calcined at 400 °C for 4 h under air flow

2.2. Catalyst characterization

The crystalline structure and the copper particle size of the different catalysts were determined by X-ray diffraction (XRD) in a Philips PW1710 BASED instrument operating at 45 kV and 30 mA, fitted with a graphite monochromator in order to get Cu Kα1 radiation (λ = 1.5406 Å); the angle step and counting time were 0.02° (2θ) and 1 s, respectively. The media copper crystal size was determined by applying the Scherrer equation.

The samples were characterized by TEM, employing a Jeol 100 CX2 (Tokyo, Japan) apparatus. Approximately one hundred gold particles were measured to perform the particle size distribution. The average diameter of the crystals in the different catalysts was calculated from the following formula: $d = (\sum n_i d_i)/n_i$. For all the cases a pre-treatment of the samples was carried out to allow the clear observation of the copper particles. The catalysts were reduced at 473 K for half an hour under H_2 flow. Afterwards, at room temperature the samples were thrown into a vessel fill with isopropanol, under gas flow. Immediately, a drop of the catalyst-solvent mixture was put on a grid and the TEM analysis was carried out.

The specific surface area of the catalysts was determined by adsorption–desorption of N_2 at 77 K employing a Nova 1200e Quantachrome equipment. The pre-treatment of the samples was an evacuation at 393 K for 20 h. The BET equation was employed for determining surface area. The diameter of the mesoporous of MCM-48 was measured by BHJ method. The choice of this method was based on previous combined TEM and BET characterization of MCM materials for determining pore sizes. The best agreement

between results from both techniques was attained following the BHJ approximation.

The TPR study was carried out in a conventional apparatus. Samples were previously calcined at 393 K in chromatographic air and purged in N_2. Afterwards, the samples were cooled down up to room temperature, and the inert gas was switched to the reactive mixture (H_2/Ar (10%)) with a flow of 18 cm³ min⁻¹. The hydrogen uptakes were measured by a TCD detector while the temperature was linearly increased at a rate of 8 K min⁻¹, up to 773 K.

The FTIR spectra of adsorbed CO were recorded in a Nicolet Nexus FTIR apparatus at 4 cm⁻¹ resolution. Catalyst samples of approximately 30–40 mg were pressed to form transparent disks of 13 mm in diameter that were mounted in a metal holder placed in the beam path. The metal holder is provided with CaF_2 windows, and coupled to a vacuum system for evacuation to 10⁻⁶ Torr. The spectra were recorded after contacting the sample with 5 Torr of CO, at 77 K.

2.3. Catalytic test

The catalysts were tested for the hydrogenation of crotonaldehyde in a Batch reactor at 373 K and 1 MPa of H_2 pressure. The reactive mixture was a 0.1 M solution of crotonaldehyde in isopropanol. Approximately 200 mg of catalyst reduced *ex situ* at 573 K were employed. The stirring rate was selected at 400 rpm. Previously, the stirring rate was varied in the range 300–900 rpm. Within this range the conversion of the CuH$_2$ catalyst was kept constant, showing the lack of external diffusion limitations.

The dependence of the conversion and of the selectivity toward the different products on time on stream was measured. The concentrations of the reactant and products were measured by gas chromatography, with a FID detector and a ZB-WAX column, at 473 K. Additionally the reaction mixture was analyzed in a PerkinElmer Clarus 500 chromatograph, provided with a mass spectrometry detector.

3. Results

The list of the Cu/MCM-48 samples is reported in Table 1.

The BET surface area of the samples is high. The lowest surface area corresponds to CuH$_5$, probably due to the fact that the relatively high copper loading partially destroys the mesoporous structure during the first step of the hydrothermal synthesis. In this way, CuH$_5$ is an heterogeneous sample, and it should be considered as a mixture of Cu/MCM-48 and Cu/SiO₂.

For the case of the hydrothermal synthesis (CuH*x*), the introduction of copper from $Cu(NO_3)_2$ corresponding to loading higher than 5%, completely destabilizes the mesoporous structure, leading to copper supported on amorphous silica.

As a general trend, the incorporation of copper in MCM-48 decreases the pore diameter (see Table 1). This effect has been previously observed for Cu/MCM-48 [13] and it could be due to different phenomena: (i) copper inserted in the silica framework, in which the heteroatom buried in the inside the walls causes the corresponding increase in the wall width and narrows the pore diameter, (ii) copper crystals with size lower than pore diameter (4.2 nm) supported inside the pores. Anyway, whatever the origin of the distortion of pore size due to the presence of copper, it is related with a high interaction between copper and the MCM-48 support.

In Fig. 1a the XRD patterns of some Cu/MCM-48 samples are shown. The strong peak centered at 2θ = 2.5° is assigned to the (2 1 1) plane. Besides other minor peaks at low diffraction angles were detected. It is interesting to note that the profile of the low diffraction peaks (see Fig. 1b) of pure MCM-48 is strongly

Table 1
Physicochemical properties of Cu/MCM-48 and Cu/SiO$_2$ catalysts.

Sample	Cu (wt%)	BET surface (m^2/g)	Pore diameter (nm)	Particle size (nm)	TPR H$_2$/Cu
MCM-48	–	1150	4.2	–	0
CuH2[c]	2.5	942	3.8	34.4[a]	0.60
CuH3	3.8	1047	3.7	29.0[a]	0.80
CuH5	5.5	423	3.7	32.1[a]	0.43
				33.2[b]	
CuI4	4.1	1004	3.8	23.1[a]	0.49
CuI10[c]	9.1	1119	3.8	25.0[a]	0.52
				26.2[b]	
CuI20	19.1	728	3.8	24.4[a]	0.72
				25.1[b]	
Cu/SiO$_2$	8.1	210	–	18.5[a]	1.1
				19.7[b]	

[a] Measured from XRD, Scherrer approximation.
[b] Measured from TEM.
[c] Samples previously reported in Ref. [13].
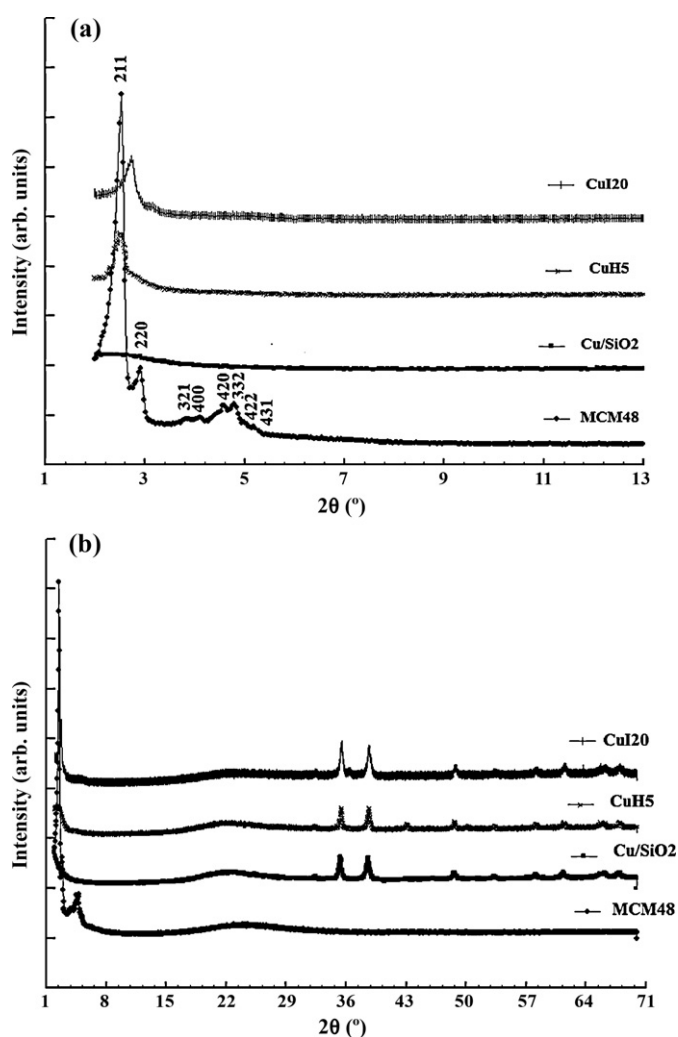
Fig. 1. (a) XRD pattern of MCM-48, C/MCM-48 and Cu/SiO$_2$; (b) a magnification for low XRD diffraction peaks.

Fig. 2. TEM micrograph of CuI20. A representative particle is signaled with an arrow.

modified in copper containing samples, showing that the incorporation of this metal in the mesoporous network is achieved. From the XRD patterns, the crystallographic parameter of pure MCM-48 and Cu/MCM-48 were determined. For the former case, the cubic unit cell parameter, a, was 85.8048 Å, while this value decreases wit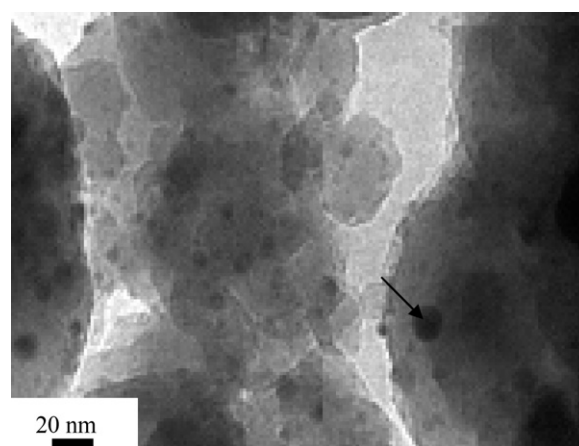h increasing the copper loading for both series. The highest the metal content, the lower the a value. To label, for CuI20, the a parameter presents the lowest value: 79.2055 Å. For CuI4 and CuI10 the values were 83.9012 and 81.3462 Å respectively. The contraction of the cell parameter would indicate the strong interaction between copper species and the MCM-48 support.

Turning the attention to the high diffraction angle peaks (see Fig. 1b), another copper phase can be identified: CuO, tenorite (2θ: 35.6 and 38.9). Thus, from the analysis of XRD diffraction peaks, it is concluded that two species are present in MCM-48: copper incorporated in the mesoporous structure of MCM-48, and supported copper crystals.

Regarding this last species, based on the width of the peak due to (1 1 1) plane, media crystallite sizes were determined by the Scherrer equation. The Warren approximation was employed for correcting instrumental line broadening. The values of crystal sizes are in the 24.4–34.4 nm range and are reported in Table 1. The trend indicates that copper particle size is higher for the CuHx samples than for CuIx.

TEM characterization of the Cu/SiO$_2$ sample indicated that the particle size, d, 19.7 nm. This result is in quite agreement with that obtained from Scherrer approximation (see Table 1). For the high loaded Cu/MCM-48 samples, CuI10, CuI20 (see Fig. 2) and CuH5, the particle sizes obtained from TEM are reported in Table 1. For these three samples, a quite good agreement between the results from TEM and those obtained from Scherrer calculations is obtained. For the low loaded Cu/MCM-48 (CuH2, CuH3 and CuI4) it was not possible to observe a considerable amount of copper particles from TEM
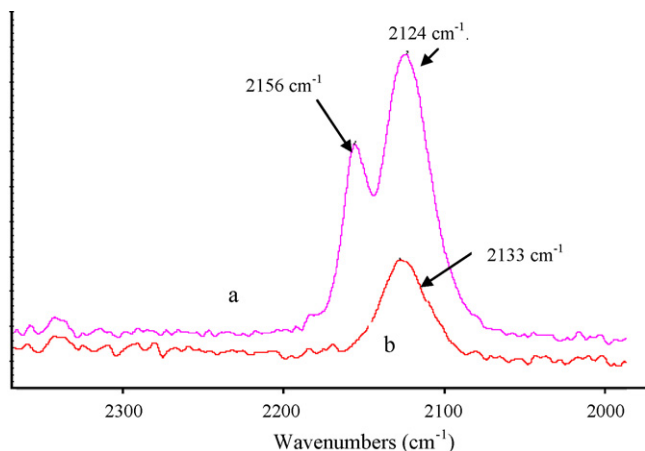
Fig. 3. FTIR spectra of CO adsorbed on previously reduced CuH5;(a) 5 Torr of CO, (b) evacuation of 15 min at 10^{-6} Torr.

Fig. 4. FTIR spectra of CO adsorbed on previously reduced Cu/SiO_2. (a) 5 Torr of CO, (b) evacuation of 15 min at 10^{-6} Torr.

micrographs. This difficulty arises from the fact that the concentration of copper particles is low for these samples. For this reason a reliable histogram could not obtained. However, it is important to note that the observed copper crystals showed a size in the 20–30 nm range.

Samples were characterized by means of TPR, in order to study the reducibility of copper in MCM-48. Slight differences in the temperature corresponding to the maxima of the consumption peak were detected (513–543 K).

If the total reduction of CuO to Cu^0 is considered, the theoretical consumption of hydrogen, expressed as mole of gas consumed per mole of copper is the unity. Cu/SiO_2 showed a hydrogen consumption similar to the theoretical one. On the contrary, the Cu/MCM-48 catalysts showed consumptions lower than the theoretical value, showing that not all copper species are being reduced. The relative low reducibility of Cu/MCM-48 would be related with copper incorporated in MCM-48 walls that is not being reduced during the TPR experiment. We will revert to this matter latter, following the FTIR characterization.

In a previous work dealing with copper supported catalysts, we have concluded on the presence of Cu^+ species in MCM-48 [15], based on a characterization carried out with FTIR of adsorbed CO. In order to further investigate on the chemical nature of copper species present in both CuH*x* and CuI*x* catalysts, a similar study was performed for the present samples. Fig. 3a shows the spectrum of adsorbed CO corresponding to the CuH5 sample previously reduced *in situ* at 573 K (the same temperature as the pre-treatment of the catalysts before catalytic testing), while Fig. 3b corresponds to the result following an evacuation at 10^{-6} Torr. The spectrum in Fig. 3a shows bands at 2156 and 2124 cm^{-1}, corresponding to CO on sylanol groups of MCM-48 and to CO on Cu^0 respectively [16,17]. After evacuating the analysis chamber only one band at 2133 cm^{-1} is observed, assigned to a strongly CO linearly bonded on Cu^+ sites [16–18]. Similar FTIR results were obtained for the other Cu/MCM-48 catalysts. For Cu/SiO_2 the spectrum of the previously reduced sample present a band at 2109 cm^{-1} due to CO bonded to Cu^0 (see Fig. 4). The interaction between CO and Cu^0 is low and after evacuating the band disappeared. No band associated with Cu^+ species was detected. The absence of Cu^+ species in Cu/SiO_2 is related with the fact that copper is completely reduced in this catalysts (TPR results). On the contrary Cu^+ species, in Cu/MCM-48 are resistant to reduction and they are not sensed in TPR experiments.
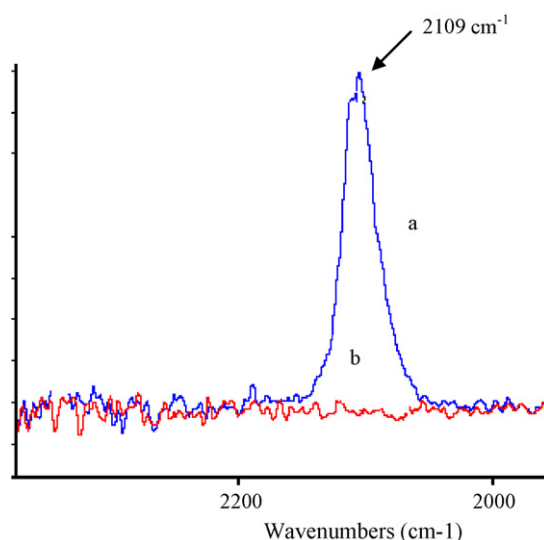
3.1. Catalytic test

The Cu/MCM-48 and the Cu/SiO_2 samples were evaluated for the selective hydrogenation of crotonaldehyde in liquid phase. In a typical run, the catalysts are pretreated *ex situ* in a glass tube, in flowing H_2 at 573 K, before introducing the sample into the reactor under the gas flow.

Firstly the external diffusion limitation effects were evaluated by varying the catalyst mass. The absence of external diffusion limitations was confirmed for catalyst weights in the 0.3–1.5 g range.

The dependence of the conversion of crotonaldehyde on time for CuI20 and Cu/SiO_2 are shown in Figs. 5 and 6 respectively. No deactivation with time on stream was observed. This result is worth to note since deactivation process are commonly observed in liquid phase hydrogenation of α,β-unsaturated compounds. We will revert to this mater later.

Another interesting point regards the reuse of the samples. Following 3 h of reaction, the CuI20 sample was separated from the reaction media, washed with fresh solvent and submitted to a new hydrogenation test. Spent CuI20 showed a similar catalytic pattern than the corresponding fresh sample. The test over the spent sample can be carried out three times without observing noticeable difference.

The specific activity for the hydrogenation of crotonaldehyde of the different samples is reported in Table 2, as moles converted per
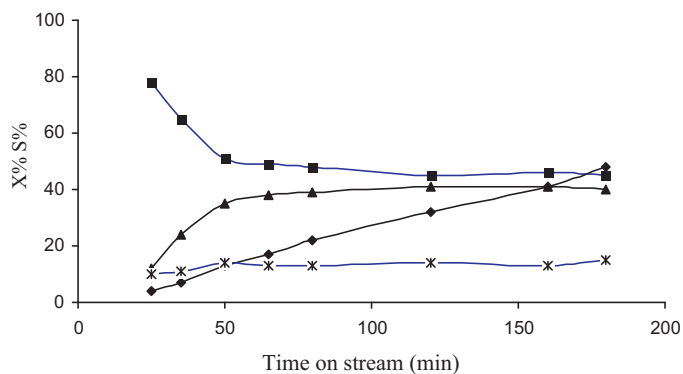

Fig. 5. Dependence on time of (♦) conversión of crotonaldehide, (■) selectivity to crotyl alcohol, (▲) butanal, (*) butanol for CuI20.
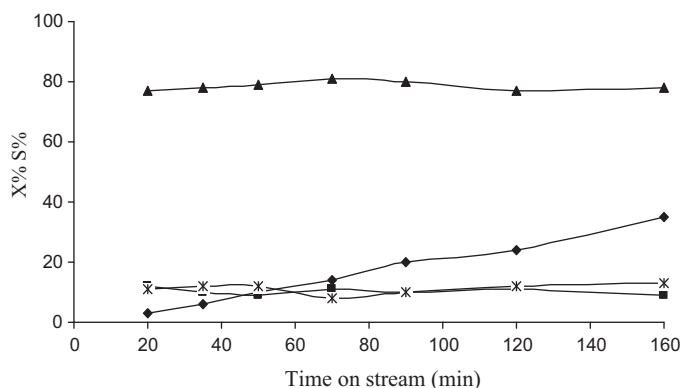
Fig. 6. Dependence on time of (♦) conversión of crotonaldehyde, (■) selectivity to crotyl alcohol, (▲) butanal, (*) butanol for Cu/SiO$_2$.

Table 2
Specific activity and selectivities to crotyl alcohol of conversion for Cu/MCM-48 and Cu/SiO$_2$.

Catalyst	Activity (μmol s^{-1} g Cu^{-1})	TOF $\times 10^3$ s^{-1}	S_{10}%[a]	S_{30}%[b]
CuH3	1.3	1.5	53	–
CuH5	0.9	1.1	55	–
CuI4	1.1	1.3		
CuI10	1.9	2.0	46	42
CuI20	1.8	1.8	48	40
Cu/SiO$_2$	3.2	3.0	7	6

[a] Selectivity to crotyl alcohol measured at 10% of conversion.
[b] Selectivity to crotyl alcohol measured at 30% of conversion.

gram of copper and per second. CuI20 and Cu/SiO$_2$ show quite similar copper particle size (see Table 1), however the specific activity of the former is approximately the half of the one corresponding to the latter sample.

TOF numbers of the catalysts are also reported in Table 2. For calculating these values, the copper surface concentration, as Cu atoms/m^2, was estimated considering the surface density of copper [19] and the particle size (as determined from TEM). The TOF numbers of all the Cu/MCM-48 catalysts were lower than the one corresponding to Cu/SiO$_2$, showing that copper supported on the mesoporous oxide is less active than when supported on silica. It is likely that a fraction of copper in the MCM-48 samples is inactive for the dissociation of dihydrogen, and in this way the activity of the samples is relatively low.

The product distribution was monitored as the conversion increased with time. Only the primary hydrogenation products of crotonaldehyde were detected. Decarbonylation did not take place nor for Cu/MCM-48 neither for Cu/SiO$_2$. Besides, condensation reactions were not detected. On the other hand, both decarbonilation and condensation reactions were observed for noble metal based catalysts tested for the hydrogenation of crotonaldehyde under similar reaction conditions [20–22]. Probably the absence of the decarbonilation reaction, which produces CO is related with the stability of copper samples in the reaction media. CO is responsible for the poisoning of metals surface and concomitantly of catalysts deactivation in liquid phase hydrogenation of α,β-unsaturated compounds [23].

Cu/SiO$_2$ should be considered an unselective catalyst, since it preferentially hydrogenates the olefinic bond. The selectivity toward crotyl alcohol is lower than 10% for all the time on stream (see Fig. 5).

On the other hand the Cu/MCM-48 catalysts were quite selective, mainly for early reaction times, at low conversion values. Selectivities toward crotyl alcohol in the 70–80% range were obtained at low conversion levels. To label, CuI20 reached a selectivity as high as 80%. The desired selectivity diminishes with time

on stream, though it is always higher than the values corresponding to Cu/SiO$_2$.

The comparison between the selectivities to crotyl alcohol of CuI20 and Cu/SiO$_2$, at the same level of conversion (10%), shows that copper supported on MCM-48 is much more selective than when supported on silica (see Table 2). Both supports are inert ones, without redox or acid–base properties. Thus, in a first approximation, no direct promotion on copper should be expected. It is likely that copper incorporated in the MCM-48 structure is related with the higher selectivity toward crotyl alcohol. Crotonaldehye would be adsorbed on this copper species in a "selective" way, by interaction of C=O bond with copper centers within the MCM-48 wall.

The CuH3, CuH5, CuI4 and CuI10 samples showed similar catalytic patterns as those observed for CuI20. In Table 2 the specific activities, TOFs number and selectivities to crotyl alcohol are reported.

4. Discussion

Cu/MCM-48 catalysts with metal loading up to 20 wt% were prepared following two different methods (hydrothermal synthesis or wet impregnation with Cu(AcAc)$_2$). The catalysts present two copper phases, which have been represented in the model proposed for Cu/MCM-48 in Fig. 7. One of them corresponds to copper incorporated within the walls of MCM-48 or highly dispersed inside the mesopores. This species would be formed during the very first step of the preparation of Cu/MCM-48 by the hydrothermal synthesis. It cannot be detected from TEM or by XRD, due to the fact that its size is lower than the detection limit of these techniques. However, this highly dispersed copper species originates a deformation of low XRD diffraction peaks of (2 1 1) planes, a contraction of the pore diameter, a variation of the crystallographic a parameter and a decreased reduction of the samples.

The other copper phase in the Cu/MCM-48 catalysts corresponds to copper crystals, with sizes in the 34–18 nm range approximately. The presence of bulky copper is clearly determined from XRD and TEM analysis, which leads to quite similar results of the corresponding sizes.

The scheme in Fig. 7 would also be a representation for the CuIx series, prepared by wet impregnation. It is rather difficult to explain the way copper is incorporated in the mesoporous wall following the wet impregnation with Cu(AcAc)$_2$, before removing the directing agent CTBA. However the existence of copper incorporated in the MCM-48 structure can be concluded based on XRD, BET and TPR characterization results, since the same modifications observed for the CuHx series were observed for the CuIx samples.

A difference between the CuIx and the CuHx series is that the size of copper crystals is higher for the catalysts prepared following the hydrothermal synthesis than for the ones prepared by wet impregnation with Cu(AcAc)$_2$. It could be considered that the affinity of the organic directing agent (CTBA) toward acetyl acetonate favors copper dispersion on the mesoporous surface.

Particular catalytic features arise due to the presence of copper species incorporated into MCM-48. TPR results showed a low specific consumption of H$_2$ of Cu/MCM-48 by comparison with Cu/SiO$_2$. It is considered that copper incorporated in MCM-48 is not being reduced in during TPR experiment, and it remains in the +1 oxidation state even after reducing the samples. Concomitantly, the pre-treatment of the catalysts before performing the catalytic test only reduces copper crystals. Taking in mind that the activation of H$_2$ takes place only on metallic surface [24], copper incorporated in the walls would remain inactive for H$_2$ dissociation, originating a lower specific activity for Cu/MCM-48 than for Cu/SiO$_2$. This would be the reason why TOF numbers of Cu/MCM-48 calculated on the basis of the total amount of copper are lower than the ones

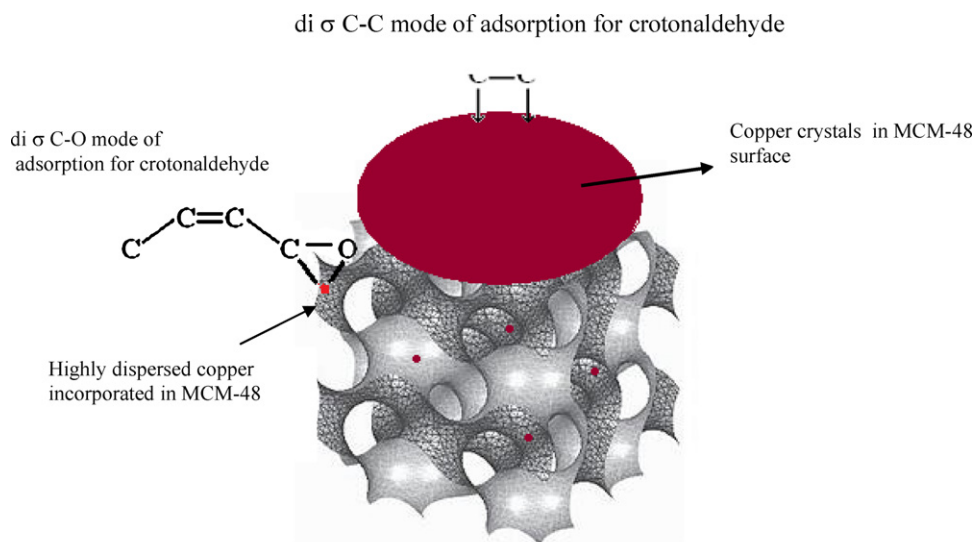di σ C-C mode of adsorption for crotonaldehyde

Fig. 7. Representation of a selective Cu/MCM-48 catalysts, showing different modes of adsorption of crotonaldehyde.

corresponding to copper supported on silica (see Table 2). On the contrary, if TOF calculations are performed on the basis of reducible copper crystals, excluding highly dispersed copper incorporated in MCM-48, the TOF values should increase. It can be speculated that the amount of reducible copper, as measured by TPR, represents only active copper species. Thus, TOF values can be recalculated giving rise to relatively high values. To label, for the CuI4 sample, only a half of copper species are active (TPR results indicated a 0.49 fraction of copper being reduced) and the TOF number of 1.1×10^{-3} increases to 2.7×10^{-3}, being this last value quite similar to the one corresponding to Cu/SiO_2. The same trends are observed for the rest of the Cu/MCM-48 catalysts. These last considerations confirm the model of the catalyst for Cu/MCM-48.

From the comparison of the selectivities toward crotyl alcohol achieved by Cu/MCM-48 and Cu/SiO_2, it should be considered that the mesoporous catalysts are selective ones. It is likely that the adsorption of crotonaldehyde occurs over the metal incorporated in the MCM-48 wall in a "selective" way, via C=O (see Fig. 6). This particular way of adsorption increases the rate of hydrogenation of the carbonyl group by comparison with the olefinic one.

The selective copper site on MCM-48 shows another interesting feature: CO is strongly bonded to it. Strong CO–Cu^+ interaction still remain upon an evacuation of the analysis chamber, showing that a stable CO-copper bond is formed. It is well known that CO forms a stable complex with copper in the +1 oxidation state, for this reason the presence of Cu^+ in all the MCM-48 samples is concluded. This species would correspond to the "selective" site for hydrogenation of carbonyl bonds. Unselective copper catalysts, as Cu/SiO_2, give quite different FITR spectra, without strongly bonded CO. Previously, it has been concluded that the presence of Cu^+ is of paramount importance for the catalytic performance of copper based catalysts, whatever the nature of the reaction. For the crotonaldehyde hydrogenation, the higher selectivity of copper based catalysts modified with sulfur species was assigned to the presence of the Cu^0–Cu^+ couple [25–27]. Besides, for the same reaction, Dandekar et al. found that the specific activity of copper based catalysts depends on the $Cu^0/(Cu^0/Cu^+)$ fraction [28].

The copper crystals supported on MCM-48 should be considered as unselective for the hydrogenation of crotonaldehyde, since they are not different from the copper crystals supported on silica (Cu/SiO_2), which favor olefinic hydrogenation. Crotonaldehyde

would be adsorbed in the di σ C–C mode on copper crystals (see Fig. 7) leading to undesired butanal. However, copper crystals are responsible for the dissociation of H_2 and therefore for the activity of the samples.

5. Conclusion

Selective copper catalysts for the hydrogenation of crotonaldehyde can be obtained by incorporating this metal in MCM-48. The copper species incorporated in the mesoporous structure would activate the C=O bond of crotonaldehyde, thus increasing the rate of carbonyl bond hydrogenation. Copper crystals, also present in MCM-48, are necessary for developing catalytic activity, though being poorly selective for crotyl alcohol production.

References

[1] B. Chou, J.L. Tsai, S. Cheng, Microporous Mesoporous Mater. 48 (2001) 309.
[2] L. Noreña-Franco, I. Hernandez-Perez, J. Aguilar-Pliego, A. Maubert-Franco, Catal. Today 75 (2002) 189–195.
[3] H. Fujiyama, I. Kohara, K. Iwai, S. Nishiyama, S. Tsuruya, M. Masaiz, J. Catal. 188 (1999) 417–425.
[4] C.L. Tsai, B. Chou, S. Cheng, J.F. Lee, Appl. Catal., A 208 (2001) 279–289.
[5] H.T. Gomes, P. Selvam, S.E. Dapurkar, J.L. Figueiredo, J.L. Faria, Microporous and Mesoporous Mater. 86 (2005) 287–294.
[6] W.B. Li, M. Zhuang, J.X. Wang, Catal. Today 137 (2008) 340–344.
[7] K. Chakarova, G. Petrova, M. Dimitrov, L. Dimitrov, G. Vayssilov, T. Tsoncheva, K. Hadjiivanov, Appl. Catal. B: Environ. 106 (2011) 186–194.
[8] P. Karandikar, A.J. Chandwadkar, M. Agashe, N.S. Ramgir, S. Sivasanker, Appl. Catal. A: Gen. 297 (2006) 220–230.
[9] B. Li, J. Wang, J. Li, Y. Xu, J. Fu, W. Yao, G. Zi, W. Wang, J. Wang, Catal. Commun. 10 (2009) 1599–1603.
[10] M. Ghadiri, F. Farzaneh, M. Ghandi, M. Alizadeh, J. Mol. Catal. A: Chem. 233 (2005) 127–131.
[11] T. Tsoncheva, Tz Venkov, M. Dimitrov, C. Minchev, K. Hadjiivanov, J. Mol. Catal. A: Chem. 209 (2004) 125–134.
[12] Ji Man Kim, Seong Kyun Kim, Ryong Ryoo, Chem. Commun. 259 (1998).
[13] V. Gutiérrez, A. Diez, M. Dennehy, M. Volpe, Microporous Mesoporous Mater. 141 (2011) 201–213.
[14] J. Xu, Z. Luan, H. He, W. Zhou, L. Kevan, Chem. Mater. 10 (1998) 3690–3698.
[15] V. Gutierrez, A. Alvarez, M. Volpe, Appl. Catal. A: Gen. 413–414 (2012) 358–365.
[16] K. Hadjiivanov, T. Tsoncheva, M. Dimitrov, C. Minchev, H. Knözinger, Appl. Catal. A: Gen. 241 (2003) 331–340.
[17] K. Hadjiivanov, M. Kantcheva, D. Klissurski, J. Chem. Soc. Faraday Trans. 92 (1996) 4595–4600.
[18] A. Davydov, A. Budneva, React. Kinet. Catal. Lett. 25 (1984) 121.
[19] Th.J. Osinga, B.G. Linsen, W.P. van Beet, J. Catal. 7 (1967) 277–279.

[20] B. Campo, S. Ivanova, C. Gigola, C. Petit, M. Volpe, Catal. Today 133 (2008) 661–666.
[21] B. Campo, C. Petit, M. Volpe, J. Catal. 254 (2008) 71–80.
[22] B. Campo, M. Volpe, C. Gigola, Ind. Eng. Chem. Res. 48 (2009) 10234–10239.
[23] M. Englisch, V. Ranade, J. Lercher, Appl. Catal. A: Gen. 163 (1997), 111.
[24] R.H. Bradley, Appl. Surf. Sci. 90 (1995) 271.
[25] G. Hutchings, F. King, I. Okoye, C. Rochester, Appl. Catal 83 (1992) L7–L13.
[26] G. Hutchings, F. King, I. Okoye, M. Padley, C. Rochester, J. Catal. 148 (1994) 453–463.
[27] G. Hutchings, F. King, I. Okoye, M. Padley, C. Rochester, J. Catal. 148 (1994) 464–469.
[28] A. Dandekar, R. Baker, M. Vannice, J. Catal. 184 (1999) 421–439.